

## Large Matter Effects in $\nu_\mu \rightarrow \nu_\tau$ Oscillations

Raj Gandhi,<sup>1</sup> Pomita Ghoshal,<sup>1</sup> Srubabati Goswami,<sup>1</sup> Poonam Mehta,<sup>2,1</sup> and S. Uma Sankar<sup>3</sup>

<sup>1</sup>Harish-Chandra Research Institute, Chhatnag Road, Jhansi, Allahabad 211 019, India

<sup>2</sup>Department of Physics and Astrophysics, University of Delhi, Delhi 110 019, India

<sup>3</sup>Department of Physics, I. I. T., Powai, Mumbai 400 076, India

(Received 13 September 2004; published 9 February 2005)

We show that matter effects change the  $\nu_\mu \rightarrow \nu_\tau$  oscillation probability by as much as 70% for certain ranges of energies and path lengths. Consequently, the  $\nu_\mu \rightarrow \nu_\mu$  survival probability also undergoes large changes. A proper understanding of  $\nu_\mu$  survival rates must consider matter effects in  $P_{\mu\tau}$  as well as  $P_{\mu e}$ . We comment on (a) how these matter effects may be observed and the sign of  $\Delta_{31}$  determined in atmospheric neutrino measurements and at neutrino factories, and (b) how they lead to heightened sensitivity for small  $\theta_{13}$ .

DOI: 10.1103/PhysRevLett.94.051801

PACS numbers: 14.60.Pq, 13.15.+g, 14.60.Lm

Two of the most outstanding problems in neutrino physics are the determination of the mixing angle  $\theta_{13}$  [1] and the sign of the atmospheric neutrino mass difference  $\Delta_{31}$  [4]. A knowledge of these parameters is crucial for understanding the form of the neutrino mass matrix. So far, most studies have concentrated on the  $\nu_\mu \rightarrow \nu_e$  oscillation probability  $P_{\mu e}$  as the means of determining the above parameters [6]. This is because the passage of neutrinos through Earth matter dramatically changes  $P_{\mu e}$ .

In this Letter we point out that the  $\nu_\mu \rightarrow \nu_\tau$  oscillation probability  $P_{\mu\tau}$  can also undergo significant change (a reduction as high as  $\sim 70\%$  or an increase of  $\sim 15\%$ ) compared to its vacuum values over an observably broad band in energies and baselines due to matter effects. This can also induce appreciable changes in the muon neutrino survival probability  $P_{\mu\mu}$  in matter.

The muon survival rate is the primary observable in iron calorimeter detectors like MINOS [7] and the proposed MONOLITH [8] and INO [9], and a major constituent of the signal in SuperKamiokande (SK) [5], the planned BNL-HomeStake [10] large water Cerenkov detector, and several detectors considered for future long baseline facilities. The  $\tau$  appearance rate as a signal for matter effects can also be searched for in special  $\tau$  detectors being thought of for neutrino factories [11]. We show that the energy ranges and baselines over which these effects occur are relevant for both atmospheric [12] and beam source neutrinos for the above experiments. Since all matter effects sensitively depend on the sign of  $\Delta_{31}$  and on  $\theta_{13}$ , observation of the effects discussed here would provide information on these important unknowns.

Our discussion below uses the approximation of constant density and sets  $\Delta_{21} \equiv \Delta_{\text{sol}} = 0$ . Consequently the mixing angle  $\theta_{12}$  and the  $CP$  phase  $\delta$  drop out of the oscillation probabilities. This simplifies the analytical expressions and facilitates the qualitative discussion of matter effects. We have checked that this works well (up to a few percent) at the energies and length scales relevant

here. However, all the plots presented in this Letter are obtained by numerically solving the full three flavor neutrino propagation equation assuming the Preliminary Reference Earth Model (PREM) [13] density profile for the Earth. Further, these numerical calculations assume  $\Delta_{21} = 8.2 \times 10^{-5} \text{ eV}^2$ ,  $\sin^2\theta_{12} = 0.27$  [14], and  $\delta = 0$  [15]. We consider matter effects in neutrino probabilities only but discuss both the cases  $\Delta_{31} = \pm|\Delta_{31}|$ . We find that dramatic matter effects occur only for  $\Delta_{31} > 0$ .

*Review of  $P_{\mu e}$  in matter.*—In vacuum, the  $\nu_\mu \rightarrow \nu_e$  oscillation probability is

$$P_{\mu e}^{\text{vac}} = \sin^2\theta_{23}\sin^22\theta_{13}\sin^2(1.27\Delta_{31}L/E), \quad (1)$$

where  $\Delta_{31} \equiv m_3^2 - m_1^2$  is expressed in  $\text{eV}^2$ ,  $L$  in km, and  $E$  in GeV. In the constant density approximation, matter effects can be taken into account by replacing  $\Delta_{31}$  and  $\theta_{13}$  in Eq. (1) by their matter dependent values,

$$\Delta_{31}^m = \sqrt{(\Delta_{31} \cos 2\theta_{13} - A)^2 + (\Delta_{31} \sin 2\theta_{13})^2} \quad (2)$$

$$\sin 2\theta_{13}^m = \sin 2\theta_{13} \Delta_{31} / \Delta_{31}^m$$

where  $A = 2\sqrt{2}G_F n_e E$  is the Wolfenstein term. The resonance condition is  $A = \Delta_{31} \cos 2\theta_{13}$ , which gives  $E_{\text{res}} = \Delta_{31} \cos 2\theta_{13} / 2\sqrt{2}G_F n_e$ . Naively, one would expect  $P_{\mu e}^{\text{mat}}$  to be maximum at  $E = E_{\text{res}}$  since  $\sin 2\theta_{13}^m = 1$ . But this is not true in general because at this energy  $\Delta_{31}^m$  takes its minimum value of  $\Delta_{31} \sin 2\theta_{13}$  and  $P_{\mu e}^{\text{mat}}$  remains small for path lengths of  $L \leq 1000$  km.  $P_{\mu e}^{\text{mat}}$  is maximum when both  $\sin 2\theta_{13}^m = 1$  and  $\sin^2(1.27\Delta_{31}^m L/E) = 1 = \sin^2[(2p+1)\pi/2]$  are satisfied. This occurs when  $E_{\text{res}} = E_{\text{peak}}^{\text{mat}}$ . This gives the condition [16]

$$[\rho L]_{\mu e}^{\text{max}} \simeq \frac{(2p+1)\pi 5.18 \times 10^3}{\tan 2\theta_{13}} \text{ km gm/cc}. \quad (3)$$

Here,  $p$  takes integer values. This condition is independent of  $\Delta_{31}$  but depends sensitively on  $\theta_{13}$ . Using the product  $\rho_{\text{av}} L$  vs  $L$  for the Earth (calculated using the PREM

profile), where  $\rho_{\text{av}}$  is the average density for a given baseline  $L$ , we identify the particular values of  $\rho_{\text{av}}L$  which satisfy Eq. (3) with  $p = 0$  for three different values of  $\sin^2 2\theta_{13}$ . These occur at  $L \simeq 10\,200$ ,  $7\,600$ , and  $11\,200$  km for  $\sin^2 2\theta_{13} = 0.1, 0.2$ , and  $0.05$ , respectively. Note that  $p = 0$  is the only relevant value of  $p$  in this case, given Earth densities and baselines [17].

*Matter effects in  $P_{\mu\tau}$ .*—In vacuum we have

$$\begin{aligned} P_{\mu\tau}^{\text{vac}} &= \cos^4 \theta_{13} \sin^2 2\theta_{23} \sin^2(1.27 \Delta_{31} L/E), \\ &= \cos^2 \theta_{13} \sin^2 2\theta_{23} \sin^2(1.27 \Delta_{31} L/E) - \cos^2 \theta_{23} P_{\mu e}^{\text{vac}}. \end{aligned} \quad (4)$$

Including the matter effects [18] changes this to

$$\begin{aligned} P_{\mu\tau}^{\text{mat}} &= \cos^2 \theta_{13}^m \sin^2 2\theta_{23} \sin^2[1.27(\Delta_{31} + A + \Delta_{31}^m)L/2E] \\ &\quad + \sin^2 \theta_{13}^m \sin^2 2\theta_{23} \sin^2[1.27(\Delta_{31} + A - \Delta_{31}^m)L/2E] \\ &\quad - \cos^2 \theta_{23} P_{\mu e}^{\text{mat}}. \end{aligned} \quad (5)$$

Compared to  $P_{\mu e}^{\text{mat}}$ , the matter dependent mass eigenstates here have a more complicated dependence on the  $\nu_\mu$  and  $\nu_\tau$  flavor content. Labeling the vacuum mass eigenstates as  $\nu_1, \nu_2$ , and  $\nu_3$ , in the approximation where  $\Delta_{21} = 0$ ,  $\nu_1$  can be chosen to be almost entirely  $\nu_e$  and  $\nu_2$  to have no  $\nu_e$  component. Inclusion of the matter term  $A$  leaves  $\nu_2$  untouched but gives a nonzero matter dependent mass to  $\nu_1$ . As the energy increases, the  $\nu_e$  component of  $\nu_1^m$  decreases and the  $\nu_\mu, \nu_\tau$  components increase such that at resonance energy they are 50%. Similarly, increasing energy increases the  $\nu_e$  component of  $\nu_3^m$  (and reduces  $\nu_\mu, \nu_\tau$  components) so that at resonance it becomes 50%. Thus in the resonance region, all three matter dependent mass eigenstates  $\nu_1^m, \nu_2^m$ , and  $\nu_3^m$  contain significant  $\nu_\mu$  and  $\nu_\tau$  components. We seek ranges of energy and path lengths for which there are large matter effects in  $P_{\mu\tau}$ , i.e., for which  $\Delta P_{\mu\tau} = P_{\mu\tau}^{\text{mat}} - P_{\mu\tau}^{\text{vac}}$  is large. We show that this occurs for two different sets of conditions, leading in one case to a decrease from a vacuum maximum and in another to an increase over a broad range of energies.

(i) *Large decrease in  $P_{\mu\tau}^{\text{mat}}$  in the resonance region.*—At energies appreciably below resonance, the  $\cos^2 \theta_{13}^m$  term in Eq. (5)  $\approx P_{\mu\tau}^{\text{vac}}$  (since  $\theta_{13}^m = \theta_{13}, A \ll \Delta_{31}, \Delta_{31}^m \approx \Delta_{31}$ ) and the  $\sin^2 \theta_{13}^m$  term is nearly zero. As we increase the energy and approach resonance,  $\cos^2 \theta_{13}^m$  begins to decrease sharply, while  $\sin^2 \theta_{13}^m$  increases rapidly. However, if resonance is in the vicinity of a vacuum peak, then the decrease in the  $\cos^2 \theta_{13}^m$  term has a much stronger impact on  $P_{\mu\tau}^{\text{mat}}$  than the increase in the  $\sin^2 \theta_{13}^m$  term, since the latter starts out at zero while the former is initially close to its peak value ( $\approx 1$ ). As a result,  $P_{\mu\tau}^{\text{mat}}$  falls sharply. This fall is enhanced by the third term in Eq. (5), which is essentially  $0.5 \times P_{\mu e}^{\text{mat}}$  (which is large due to resonance), leading to a large overall drop in  $P_{\mu\tau}^{\text{mat}}$  from its vacuum value. Note that the requirement that we be at a vacuum peak to begin with

forces  $\Delta P_{\mu\tau}$  to be large and negative, with the contributions from the first and the third term reinforcing each other.

The criterion for maximal matter effect,  $E_{\text{res}} \approx E_{\text{peak}}^{\text{vac}}$ , leads to the following condition:

$$[\rho L]_{\mu\tau}^{\text{max}} \simeq (2p + 1)\pi 5.18 \times 10^3 (\cos^2 \theta_{13}) \text{ km gm/cc}. \quad (6)$$

Unlike Eq. (3), which has a  $\tan 2\theta_{13}$  in its denominator, Eq. (6) has a much weaker dependence on  $\theta_{13}$ . This enables one to go to a higher value of  $p$  without exceeding the baselines relevant for observing Earth matter effects. Incorporating the  $E_{\text{res}} = E_{\text{peak}}^{\text{vac}}$  condition we get  $\Delta P_{\mu\tau}$  as

$$\Delta P_{\mu\tau} \simeq \cos^4 [\sin 2\theta_{13} (2p + 1) \frac{\pi}{4}] - 1, \quad (7)$$

where we approximated  $\cos 2\theta_{13} \approx 1$ . We note that, in general,  $\Delta P_{\mu\tau}$  will be larger for higher values of both  $p$  and  $\theta_{13}$ . From Eq. (6), for  $p = 1$  and  $\sin^2 2\theta_{13} = 0.1(0.2, 0.05)$ ,  $E_{\text{res}} = E_{\text{peak}}^{\text{vac}}$  occurs at  $\sim 9700$  (9300, and 9900 km) and  $\Delta P_{\mu\tau} \approx -0.7$  [from Eq. (7)]. For  $p = 0$ , Eq. (6) gives  $L_{\mu\tau}^{\text{max}} \sim 4400$  km for  $\sin^2 2\theta_{13} = 0.1$ . However,  $\Delta P_{\mu\tau}$  is roughly one-tenth of the  $p = 1$  case. In general, for a given baseline, the choice of an optimal  $p$  is also dictated by the constraint that the vacuum peak near resonance have a breadth which makes the effect observationally viable.

In Fig. 1(a) we show all three matter and vacuum probabilities for 9700 km. In these plots  $\Delta_{31}$  is taken as  $0.002 \text{ eV}^2$ , which gives  $E_{\text{res}} = E_{\text{peak}}^{\text{vac}} \sim 5 \text{ GeV}$ . The middle panel of Fig. 1(a) shows that near this energy  $P_{\mu\tau}^{\text{mat}}$  ( $\sim 0.33$ ) is appreciably lower compared to  $P_{\mu\tau}^{\text{vac}}$  ( $\sim 1$ ). Thus the drop due to matter effect is 0.67, which agrees well with that obtained earlier using the approximate expression Eq. (7).

In Fig. 2 we show the  $\theta_{13}$  sensitivity of  $P_{\mu\tau}^{\text{mat}}$  at 9700 km. In particular, at  $E_{\text{res}} \approx E_{\text{peak}}^{\text{vac}}$  the strong dependence on  $\theta_{13}$  is governed by Eq. (7) above. Unlike  $P_{\mu e}^{\text{mat}}$ , where the event rate decreases as  $\theta_{13}^2$  for small values of  $\theta_{13}$ , the  $\tau$  appearance rate at  $E_{\text{res}} = E_{\text{peak}}^{\text{vac}}$  increases with decreasing  $\theta_{13}$ . As  $\sin^2 2\theta_{13}$  goes from 0.2 to 0,  $P_{\mu\tau}^{\text{mat}}$  varies from  $\sim 0.05$  to  $\sim 1$ . For very small values of  $\sin^2 2\theta_{13} (< 0.05)$  it will be impossible to see a maximal resonance enhancement in  $P_{\mu e}$  because the distance for which this occurs exceeds the diameter of the earth. However, the observation of resonant suppression in  $P_{\mu\tau}$  is possible, even for very small values of  $\theta_{13}$ , if the criterion,  $N_\tau(\theta_{13} = 0) - N_\tau(\theta_{13}) \geq 3[\sqrt{N_\tau(\theta_{13} = 0)} + \sqrt{N_\tau(\theta_{13})}]$ , is satisfied for the tau event rate.

In general the resonance has a width, and this fact affects observability. To include the width of the resonance, we write  $A = \Delta_{31}(\cos 2\theta_{13} + q \sin 2\theta_{13})$ . We find that the large matter effects discussed above still do occur as long as  $A$  is within the width of the resonance or  $-1 \leq q \leq 1$ .

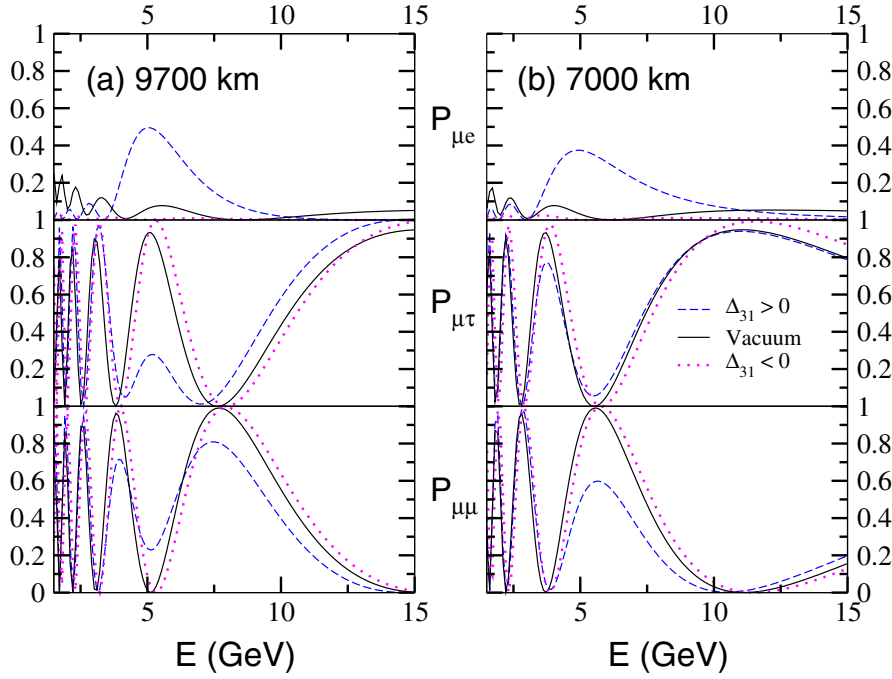


FIG. 1 (color online).  $P_{\mu e}$ ,  $P_{\mu\tau}$ , and  $P_{\mu\mu}$  plotted vs neutrino energy,  $E$  (in GeV) in matter and in vacuum for both signs of  $\Delta_{31}$  for two different baseline lengths: (a) for  $L = 9700$  km and (b) for  $L = 7000$  km. These plots use  $\Delta_{31} = 0.002$  eV<sup>2</sup> and  $\sin^2 2\theta_{13} = 0.1$ .

(ii) *Increase in  $P_{\mu\tau}$  away from resonance.*—It is also possible for  $P_{\mu\tau}^{\text{mat}}$  to differ appreciably from  $P_{\mu\tau}^{\text{vac}}$  away from resonance. This is evident in Fig. 1(a) (central panel) in the energy range 7.5–15 GeV. This effect is an enhancement rather than a drop, i.e.,  $\Delta P_{\mu\tau}$  is now positive.  $\Delta P_{\mu e}$  is small in most of the latter part of the energy region under consideration and does not contribute in an important way overall. The dominant contribution to this enhancement arises from the  $\sin^2 \theta_{13}^m$  term in  $P_{\mu\tau}$  [Eq. (5)] which is large for  $E \gg E_{\text{res}}$ . Since  $(\Delta_{31} + A - \Delta_{31}^m) \approx 2\Delta_{31}$  for these energies, we obtain an enhancement ( $\sim 15\%$ ) which follows the vacuum curve. The difference between the vacuum and matter curves largely reflects the difference between the  $\cos^4 \theta_{13}$  multiplicative term in the vacuum expression Eq. (4) and the  $\sin^2 \theta_{13}^m$  multiplicative term in Eq. (5). While this effect is smaller compared to the effect in (i) above, it occurs over a broad energy band and may manifest itself in energy integrated event rates.

Finally, we comment on the observability of the matter effects in  $P_{\mu\tau}$ . The energies in question are above, but close to the  $\tau$  production threshold. This suppresses the  $\tau$  appearance rates, and will necessitate a high luminosity beam experiment. Such direct observation must perhaps await the advent of superbeams and or neutrino factories. However, the effects in  $P_{\mu\tau}^{\text{mat}}$  manifest themselves indirectly in  $P_{\mu\mu}^{\text{mat}}$ , as we discuss below, and these can be observed in an atmospheric neutrino experiment.

*Matter effects in  $P_{\mu\mu}$ .*—The deviation of  $P_{\mu\mu}^{\text{mat}}$  from  $P_{\mu\mu}^{\text{vac}}$  clearly results from the combined effects in  $P_{\mu\tau}^{\text{mat}}$  and  $P_{\mu e}^{\text{mat}}$ , i.e.,  $\Delta P_{\mu\mu} = -\Delta P_{\mu\tau} - \Delta P_{\mu e}$ . In case (i) above, for instance,  $\Delta P_{\mu\tau}$  is large and negative while  $\Delta P_{\mu e}$  is positive and hence they do not contribute in consonance. However,

the resulting change in  $P_{\mu\mu}$  is still large, given the magnitude of the change ( $\approx 70\%$ ) in  $P_{\mu\tau}$ . This is visible in the bottom panel of Fig. 1(a), in the energy range 4–6 GeV.

One also expects a significant drop in  $P_{\mu\mu}^{\text{mat}}$  when either of  $\Delta P_{\mu\tau}$  or  $\Delta P_{\mu e}$  is large and the other one is small. The first of these cases ( $\Delta P_{\mu\tau}$  large,  $\Delta P_{\mu e}$  small) is shown in Fig. 1(a) in the energy range  $\sim 6$ –15 GeV, with the enhancement in  $P_{\mu\tau}^{\text{mat}}$  reflected in the decrease in  $P_{\mu\mu}^{\text{mat}}$ . The second case (small  $\Delta P_{\mu\tau}$  large,  $\Delta P_{\mu e}$ ) occurs when a minimum in the vacuum value of  $P_{\mu\tau}$  resides in the proximity of a resonance, and even the rapid changes in  $\sin^2 \theta_{13}^m$  and  $\cos^2 \theta_{13}^m$  in this region fail to modify this small value significantly. This condition can be expressed as  $1.27\Delta_{31}L/E = p\pi$ . Note that this corresponds to a vacuum peak of  $P_{\mu\mu}$ . Substituting  $E$  as  $E_{\text{res}}$  gives the distance for maximum matter effect in  $P_{\mu\mu}$  as

$$[\rho L]_{\mu\mu}^{\text{max}} \approx p\pi \times 10^4 (\cos 2\theta_{13}) \text{ km gm/cc.} \quad (8)$$

For  $p = 1$  this turns out to be  $\sim 7000$  km. This effect [19] is shown in the bottom panel of Fig. 1(b). The large (40% at its peak) drop in  $P_{\mu\mu}$  seen in this figure derives its strength from the resonant enhancement in  $P_{\mu e}$ . A sensitivity to  $\theta_{13}$  around the peak similar to the one discussed above for  $P_{\mu\tau}^{\text{mat}}$  also exists here, leading to a larger muon survival rate as  $\theta_{13}$  becomes smaller. The width of both these effects is significant, ranging from 4–10 GeV in the first case [Fig. 1(b)] and 6–15 GeV in the second. We have checked that they persist over a range of baselines (6000–9700 km), making them observationally feasible.

*Observational possibilities and conclusions.*—We have shown that large matter effects in neutrino oscillations are

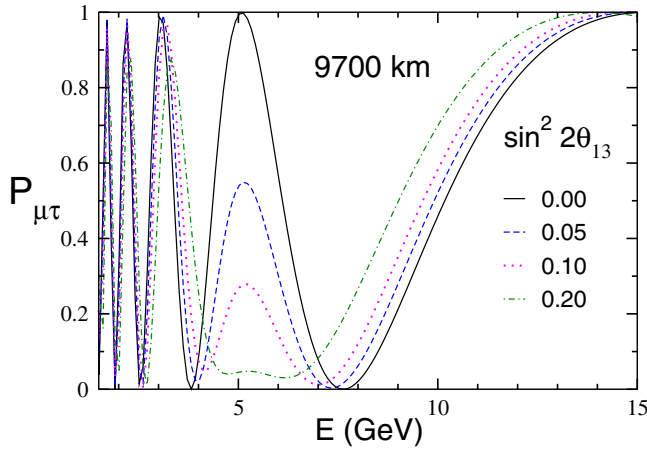


FIG. 2 (color online).  $P_{\mu\tau}$  plotted against the neutrino energy,  $E$  (in GeV) for different values of  $\theta_{13}$ . We have used  $\Delta_{31} = 0.002 \text{ eV}^2$ .

not necessarily confined to  $\nu_\mu \rightarrow \nu_e$  or  $\nu_e \rightarrow \nu_\tau$  conversions, but can be searched for in  $\nu_\mu \rightarrow \nu_\tau$  oscillation and  $\nu_\mu \rightarrow \nu_\mu$  survival probabilities. We have discussed their origin by studying the interrelations of all the three matter probabilities,  $P_{\mu e}^{\text{mat}}$ ,  $P_{\mu\tau}^{\text{mat}}$ , and  $P_{\mu\mu}^{\text{mat}}$ , and identified baseline and energy ranges where they act coherently to give observationally large effects. The effects discussed are strongly sensitive to the sign of  $\Delta_{31}$ , as is apparent in the figures above. Also, there is sensitivity to small  $\theta_{13}$  at the energy and baseline ranges identified for  $P_{\mu\tau}^{\text{mat}}$  and  $P_{\mu\mu}^{\text{mat}}$ .

Specialized  $\tau$  detectors operating in long baseline scenarios [11] should be able to observe effects like the ones discussed in the central panel of Fig. 1(a) and in Fig. 2. Similarly, detectors capable of measuring muon survival rates, e.g., magnetized iron calorimeters can detect the effects visible in the bottom panels of Fig. 1(a) and 1(b)[20]. To illustrate the observability of the effect, we calculate that for a magnetized iron calorimeter detector [8,9] and an exposure of 1000 kT yr, in the energy range 5–10 GeV and  $L$  range of 6000–9700 km, with  $\Delta_{31} = +0.002 \text{ eV}^2$  and  $\sin^2 2\theta_{13} = 0.1$ , the total number of atmospheric  $\mu^-$  events in the case of vacuum oscillations is 261. However, it reduces to 204 with matter effects. The rates for  $\mu^+$  in matter are identical to the vacuum value of 105 events. These numbers reflect a  $4\sigma$  signal for the effect discussed above for  $P_{\mu\mu}^{\text{mat}}$  [21]. The Fermilab to Kamioka proposal [22] has a baseline of 9300 km and is within the range of baselines where these effects are large and observable.

Finally, we remark that although the effects discussed here appear only for  $\nu_\mu$  for  $\Delta_{31}$  positive (and only for  $\bar{\nu}_\mu$  for  $\Delta_{31}$  negative) it may still be possible to search for them in the accumulated SK data.

P.M. acknowledges CSIR, India for partial financial support and HRI and INO for hospitality.

- 
- [1] The current bound on  $\theta_{13}$  is  $\sin^2 \theta_{13} < 0.05(3\sigma)$  [2]. However, this is sensitive to the value of  $\Delta_{31}$  [3].
  - [2] A. Bandyopadhyay *et al.* hep-ph/0406328.
  - [3] S. Goswami, hep-ph/0409224.
  - [4] The best-fit value of  $\Delta_{31}$  from zenith angle analysis of SK data is  $2.1 \times 10^{-3} \text{ eV}^2$  [5].
  - [5] E. Kearns, in *Neutrino 2004*, see, <http://neutrino2004.in2p3.fr/>.
  - [6] See, e.g., I. Mocioiu and R. Shrock, Phys. Rev. D **62**, 053017 (2000); V.D. Barger *et al.*, Phys. Rev. D **62**, 013004 (2000); V.D. Barger *et al.* Phys. Lett. B **485**, 379 (2000); E.K. Akhmedov *et al.*, J. High Energy Phys. 04 (2004) 078, and references therein.
  - [7] R. Saakian, Nucl. Phys. B, Proc. Suppl. **111**, 169 (2002).
  - [8] N.Y. Agafonova *et al.*, Report No. LNGS-P26-2000; <http://castore.mi.infn.it/~monolith/>.
  - [9] See <http://www.imsc.res.in/~ino>.
  - [10] M. Diwan *et al.*, hep-ex/0211001.
  - [11] C. Albright *et al.*, hep-ex/0008064.
  - [12] Matter effects for atmospheric neutrinos are also discussed, e.g., in E.K. Akhmedov *et al.* Nucl. Phys. B **542**, 3 (1999); J. Bernabeu *et al.*, Phys. Lett. B **531**, 90 (2002).
  - [13] We use the parametrization given in R. Gandhi *et al.*, Astropart. Phys. **5**, 81 (1996).
  - [14] KamLAND Collaboration, T. Araki *et al.*, hep-ex/0406035.
  - [15] We checked that for  $\delta = \pm\pi/2$  the change is within 10%.
  - [16] M.C. Banuls *et al.*, Phys. Lett. B **513**, 391 (2001).
  - [17] The approximation of “average constant density” is not a good one for core passage but is included here since it delineates the range of  $\sin^2 2\theta_{13}$  where core passage is a requisite for maximal matter effects.
  - [18] See the third and fourth references in [6].
  - [19] See the first reference in [6]. Also see [16] and the second reference in [20].
  - [20] T. Tabarelli de Fatis, Eur. Phys. J. C **24**, 43 (2002); S. Palomares-Ruiz and S.T. Petcov, hep-ph/0406096; D. Indumathi and M.V.N. Murthy, Phys. Rev. D **71**, 013001 (2005).
  - [21] R. Gandhi *et al.*, hep-ph/0411252.
  - [22] F. DeJongh, hep-ex/0203005.